

RESEARCH

Open Access



# The protective effect of hydrogen sulfide on systemic sclerosis associated skin and lung fibrosis in mice model

Zhi Wang<sup>†</sup>, Xiaoya Yin<sup>†</sup>, Luyan Gao, Sheng Feng, Kai Song, Lingyun Li, Ying Lu and Huaying Shen<sup>\*</sup>

## Abstract

**Background:** Systemic sclerosis (SSc) caused fibrosis can be fatal and it still lack of effective treatment. Hydrogen sulfide (H<sub>2</sub>S) appears to be an attractive therapeutic candidates. This study aimed to investigate the protective effect of H<sub>2</sub>S on SSc-associated skin and lung fibrosis.

**Methods:** We developed a model of SSc by subcutaneous injecting BLM to female C3H mice. The mice received daily subcutaneous injections of NaHS (56 and 112 μg/kg), an H<sub>2</sub>S donor. On days 7, 28, and 42, the mice were killed and blood samples were collected to measure the plasma H<sub>2</sub>S concentration, the skin and lung tissues was harvested for microscopic examination, immunohistochemistry and quantify biological parameters (hydroxyproline content, RT-qPCR and Western blot).

**Results:** In model group, the dermis of skin tissues at different time points gradually thickened, collagen deposition increased. The lung tissues presented pathological changes such as obvious inflammatory cell infiltration, increased collagen deposition and the plasma H<sub>2</sub>S concentrations points significantly decreased. Administration of NaHS markedly decreased the biomarkers of fibrosis such as α-smooth muscle actin, collagen-I, collagen-III, fibronectin, transforming growth factor-β1, Smad2/3 phosphorylation and inflammation including the marker protein of monocyte/macrophage and monocyte chemoattractant protein-1 in the lung. Compared to the low dose group, the expression in the high dose group have decreased trend, but the difference was not significant.

**Conclusion:** We demonstrate the beneficial effects of H<sub>2</sub>S on SSc-associated skin and lung fibrosis. H<sub>2</sub>S may be a potential therapy against this intractable disease.

**Keywords:** Systemic sclerosis, Fibrosis, Transforming growth factor-β1, Hydrogen sulfide

## Background

Systemic sclerosis (SSc) is a severe connective tissue disease of unknown etiology. SSc is characterized by multivisceral fibrosis resulting from inflammation, vascular injury and excessive collagen deposition. Skin sclerosis can cause discomfort and organ involvements—such as pulmonary fibrosis—can be fatal. However, the mechanisms of fibrosis in SSc have not been fully elucidated

and effective drugs are still scarce (Walker et al. 2012). Immunosuppressants, used to treat SSc, can also cause important adverse effects, such as hepatic and renal functional lesion, bone marrow depressions and infecting etc. Therefore, new therapy options need to be found.

Hydrogen sulfide (H<sub>2</sub>S) is a newly recognized endogenous gasotransmitter analogic to nitric oxide and carbon monoxide (Wang 2012). As a new emerging gaseous signalling molecule, for a long time, its study was limited to its toxicity. In the 1990s, it was discovered that endogenous H<sub>2</sub>S participated in anti-inflammation, anti-oxidation, and the regulation of cell proliferation and apoptosis (Gao et al. 2012; Moody and Calvert 2011; Vandiver and Snyder 2012). Past studies have confirmed

\*Correspondence: shenhy513@sina.com

<sup>†</sup>Zhi Wang and Xiaoya Yin contribute equally to this work and co-first authors

Department of Nephrology, Second Affiliated Hospital of Soochow University, 1055 Sanxiang Road, Jinchang, Suzhou 215000, Jiangsu Province, China

that exogenous H<sub>2</sub>S attenuates aortic-coarctation-induced cardiac hypertrophy and fibrosis (Huang et al. 2012), inhibit renal interstitial fibrosis caused by obstructive nephropathy (Song et al. 2014), relieve peritoneal mesothelial cell injury caused by high-glucose peritoneal dialysis fluids (Lu et al. 2015) and carbon tetrachloride-induced cirrhosis (Tan et al. 2011). The potential mechanisms of H<sub>2</sub>S anti-fibrotic may be account for inhibiting the activation and migration of inflammatory cells likewise myofibroblasts, subsequently decrease the production of pro-inflammatory cytokines and extracellular matrix accumulation (Li et al. 2008; Tan et al. 2011). Therefore, we hypothesized that H<sub>2</sub>S may against organ fibrosis caused by immune reaction. Importantly, the present of H<sub>2</sub>S in a variety of mammalian tissues and organs support it may be without overt adverse effect.

We conduct this study to investigate the effect of H<sub>2</sub>S on SSc-associated skin and lung fibrosis in mice model established by subcutaneous injections with BLM, and also examined the underlying anti-fibrotic mechanisms.

## Methods

### Establishment of animal models

After adaptive feeding for 1 week, 75 clean-grade female C3H mice with a body weight of 18–22 g (SLAC, Shanghai) were randomly divided into 5 groups: (1) control group: local subcutaneous injection of PBS 0.1 ml + intraperitoneal injection of PBS 1 ml; (2) model group: local subcutaneous injection of 1 mg/ml bleomycin (BLM, Nippon Kayaku Co. Ltd.) 0.1 ml + intraperitoneal injection of PBS 1 ml; (3) low dose treatment group: local subcutaneous injection of 1 mg/ml BLM 0.1 ml + intraperitoneal injection of 56 µg/kg/d NaHS (Sigma, USA); (4) high dose treatment group: local subcutaneous injection of 1 mg/ml BLM 0.1 ml + intraperitoneal injection of 112 µg/kg/d NaHS; (5) H<sub>2</sub>S group: local subcutaneous injection of PBS 0.1 ml + intraperitoneal injection of 112 µg/kg/d NaHS. BLM (0.1 ml) dissolved in PBS at a concentration of 1 mg/ml, was subcutaneously each day for 4 consecutive weeks. Intraperitoneal injection of 56 µg/kg/d or 112 µg/kg/d NaHS began at the same time with BLM injection and lasted for 6 weeks. Five mice in each group were randomly sacrificed on days 7, 28, and 42. Serum samples of mice were collected to measure the H<sub>2</sub>S concentrations. Skin and lung tissues of mice were collected for pathological staining using haematoxylin-eosin (HE) stain and Masson stain to observe the degrees of inflammation and fibrosis in lung tissues. The alkaline hydrolysis method was performed to determine the concentrations of hydroxyproline (HYP) in lung tissues (Jiangcheng Bioengineering Institute, Nanjing). PCR and western blot were performed to detect the expression of fibrosis indicators such as  $\alpha$ -smooth muscle

actin ( $\alpha$ -SMA), collagen-I (Col-I), collagen-III (Col-III), fibronectin (FN), transforming growth factor- $\beta$ 1 (TGF- $\beta$ 1) and Smad2/3 phosphorylation (p-Smad2/3). Immunohistochemistry was performed to detect the expression of inflammatory cytokines including the marker protein (ED-1) of monocyte/macrophage and monocyte chemoattractant protein-1 (MCP-1). The  $\alpha$ -SMA, FN and p-Smad2/3 antibodies were purchased from Santa Cruz; all other antibodies were purchased from Abcam.

### Histopathological staining

Skin tissues and left lung tissues from the injection locations in the neck and back of mice were fixed in 4 % paraformaldehyde, embedded in paraffin, and cut into 5 µm sections. HE and Masson stains were performed to observe the changes of gross morphology, inflammation, and collagen deposition.

### Measurement of the plasma H<sub>2</sub>S levels

The NaHS standard was used for a twofold serial dilution to obtain concentrations from 1.56 to 100 µM. The DNA-Az (H<sub>2</sub>S probe) was dissolved in anhydrous ethanol to obtain the final concentration of 2.2 mM. One black 96-well plate was obtained, and 10 µl of 2.2 mM DNS-Az stock solution was then added to each well followed by 100 µl fresh plasma or the NaHS standard immediately to obtain a DNS-Az concentration of 200 µM. The absorbance value of each well was measured in a microplate reader. The excitation wavelength was 360 nm, and the emission wavelength was 528 nm. The NaHS results were used to plot a standard curve. The absorbance values of plasma wells were compared with the standard curve to obtain the plasma H<sub>2</sub>S levels.

### Measurement of HYP concentration

Lung tissues of mice at a wet weight of 30–100 mg were collected. The HYP levels in lung tissues were detected using alkaline hydrolysis colorimetry. Lung tissues were hydrolysed using an alkaline solution. Chloramine T, perchloric acid, and 4-(dimethylamino) benzaldehyde were sequentially added. After mixing thoroughly, samples were incubated in a 60 °C water bath for 15 min. The samples were cooled down and centrifuged, and the supernatant was collected. The absorbance values at 550 nm wavelength and 1 cm optic path were measured. Calibration was performed using a blank tube and a standard tube. The results are presented as µg/mg.

### RT-PCR

Total RNA from right lung tissues of mice was extracted using the TRIzol method. The concentration of the total RNA was measured using a spectrophotometer.

The synthesis of cDNA was performed according to the procedures of the reverse transcription reagent kit. The primer sequences of  $\beta$ -actin,  $\alpha$ -SMA, Col-I, and Col-III were synthesized by Sangon Biotech (Shanghai). Primer sequences are shown in Table 1.

#### Western blot

The frozen right lung tissues of mice were added to the tissue lysis solution. After homogenization and centrifugation, the supernatant was collected. Protein concentrations were determined using the BCA method, and the protein samples were stored in a  $-80^{\circ}\text{C}$  freezer for future usage. A 10 % polyacrylamide gel was prepared for electrophoresis. After the samples were transferred to a membrane and blocked, the primary antibody was added (1:1000 dilution) and incubated at  $4^{\circ}\text{C}$  overnight. The secondary antibody was then added (1:5000 dilution) and incubated at room temperature for 1 h. The results were developed, and fibrosis indicators such as  $\alpha$ -SMA, FN, TGF- $\beta$ 1 and p-Smad2/3 were detected.

#### Immunohistochemistry

The streptavidin–biotin peroxidase complex (ABC) method was used for immunohistochemistry. The dilution of the primary antibodies was 1:100 for ED1 and 1:100 for MCP-1. Five fields were randomly selected under a microscope (400 $\times$ ). After the positive regions were localized, images were taken using a colour camera. The results were input into a colour image analysis system. After the positive regions were precisely segmented, the quantities of ED1 and MCP-1 positive cells were measured, and the mean values were calculated.

**Table 1 Primers for polymerase chain reaction**

cDNA	Primers	Reaction condition
$\beta$ -actin	5'-GTGCTATGTTGCTCTAGAC TTCG-3'	94 $^{\circ}\text{C}$ , 30 s; 55 $^{\circ}\text{C}$ , 30 s; 72 $^{\circ}\text{C}$ , 1 min (30)
	5'-ATGCCACAGGATTCCATAC C-3'	
$\alpha$ -SMA	5'-GGGAGTAATGGTTGGAAT GG-3'	94 $^{\circ}\text{C}$ , 30 s; 55 $^{\circ}\text{C}$ , 30 s; 72 $^{\circ}\text{C}$ , 1 min (30)
	5'-GGTGATGATGCCGTGTTT TA-3'	
Col-1	5'-TGACTGGAAGAGCGGAGA GT-3'	94 $^{\circ}\text{C}$ , 30 s; 52 $^{\circ}\text{C}$ , 30 s; 72 $^{\circ}\text{C}$ , 1 min (30)
	5'-CGGCTGAGTAGGGAACA CAC-3'	
Col-III	5'-AGGTTCTCCTGGTCTGC T-3'	94 $^{\circ}\text{C}$ , 30 s; 55 $^{\circ}\text{C}$ , 30 s; 72 $^{\circ}\text{C}$ , 1 min (30)
	5'-ATGCCCACTGTTCCATCT T-3'	

$\alpha$ -SMA  $\alpha$ -smooth muscle actin, Col-1 collagen-1, Col-III collagen-III

#### Statistical analysis

Measurement data are presented as mean  $\pm$  SD. Comparison among multiple groups was performed using one-way analysis of variance. A threshold  $\alpha = 0.05$  was used as the detection level. Data were analysed using the SPSS17.0 software.

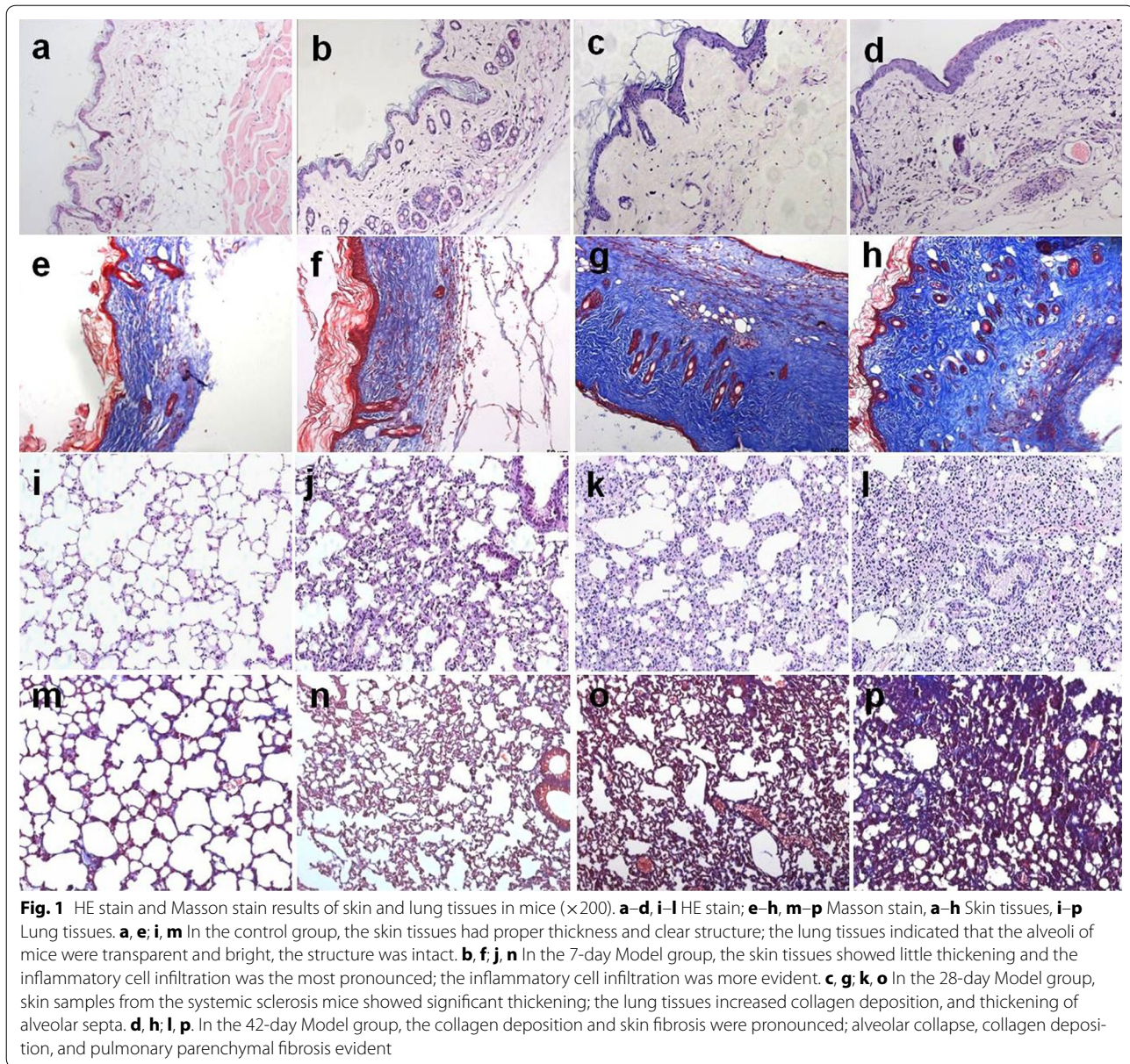
## Results

#### Pathological changes in skin tissues

HE stain and Masson stain results of skin tissues indicated that the dermis of mice in the control group had proper thickness, clear structure, and a large amount of underlying adipose tissue (Fig. 1a, e). Skin tissues of mice in the model group at different time points exhibited significant thickening of the dermis and disordered structure with increasing model establishment time there was inflammatory cell filtration and collagen deposition (Fig. 1b–d, f–h). Of these features, the inflammatory cell infiltration was the most pronounced in the 7-day group (Fig. 1b), and the collagen deposition and skin fibrosis were the more pronounced in the 28- and 42-day group (Fig. 1g, h). After NaHS intervention, the skin tissues of mice in the treatment group exhibited a clear structure, the dermis became thinner, the lipid layer thickened, inflammatory cell filtration and collagen deposition significantly decreased compared to the model group on 7-day (Fig. 2c, d) and on 42 day (Fig. 2h, i; m, n). Compared to that in the low dose treatment group, the improvement in the high dose group was even more clearly detectable (Fig. 2e, j, o).

#### Pathological changes in lung tissues

HE stain and Masson stain results of lung tissues indicated that the alveoli of mice in the control group were transparent and bright, the structure was intact (Fig. 1i, m). Compared to the control group, the model group at different time points all exhibited obvious inflammatory cell infiltration, alveolar collapse, disordered structure, increased collagen deposition, and thickening of alveolar septa (Fig. 1j–l; m, o, p). Thereinto, the inflammatory cell infiltration was more evident in the 7-day group (Fig. 1j); whereas the alveolar collapse, patchy fusion, collagen deposition, and pulmonary parenchymal fibrosis were the more evident in the 28- and 42-day group (Fig. 1o, p). After NaHS intervention, lung tissue pathological changes in mice from the treatment group were significantly relieved, inflammatory cell filtration and collagen deposition decreased, alveolar structure improved, the alveoli were more transparent and bright, and the degree of inflammation and fibrosis decreased on 7-day (Fig. 3c, d) and on 42 day (Fig. 3h, i; m, n).



### Changes in the plasma $H_2S$ concentrations

Compared to the control group, the plasma  $H_2S$  concentrations for mice in the model group at different time points all decreased. The mean plasma  $H_2S$  concentration for mice in the 7-day control group was  $24.96 \pm 4.12 \mu M$ . The concentration in the 7-day model group was  $22.79 \pm 1.54 \mu M$ ; the concentration decreased compared to that in the control group, but the difference was not statistically significant. The concentrations in the 28- and the 42-day control groups were  $24.66 \pm 3.52$  and  $24.41 \pm 2.57 \mu M$ . The concentrations in the 28-day model group and the 42-day model groups were  $18.59 \pm 3.32$

and  $16.49 \pm 2.46 \mu M$ , respectively compared to that in the control group, the differences were each statistically significant (Fig. 4).

### $H_2S$ reduces the expression level of HYP in the lung tissues of mice induced by BLM on the 42th day

Compared to that in the control group, the HYP levels in the lung tissues of mice in the model group at different time points all significantly increased. For example in the 42-day group, after NaHS intervention, the HYP concentration in the treatment group significantly decreased. The decreasing trend in the high dose treatment group

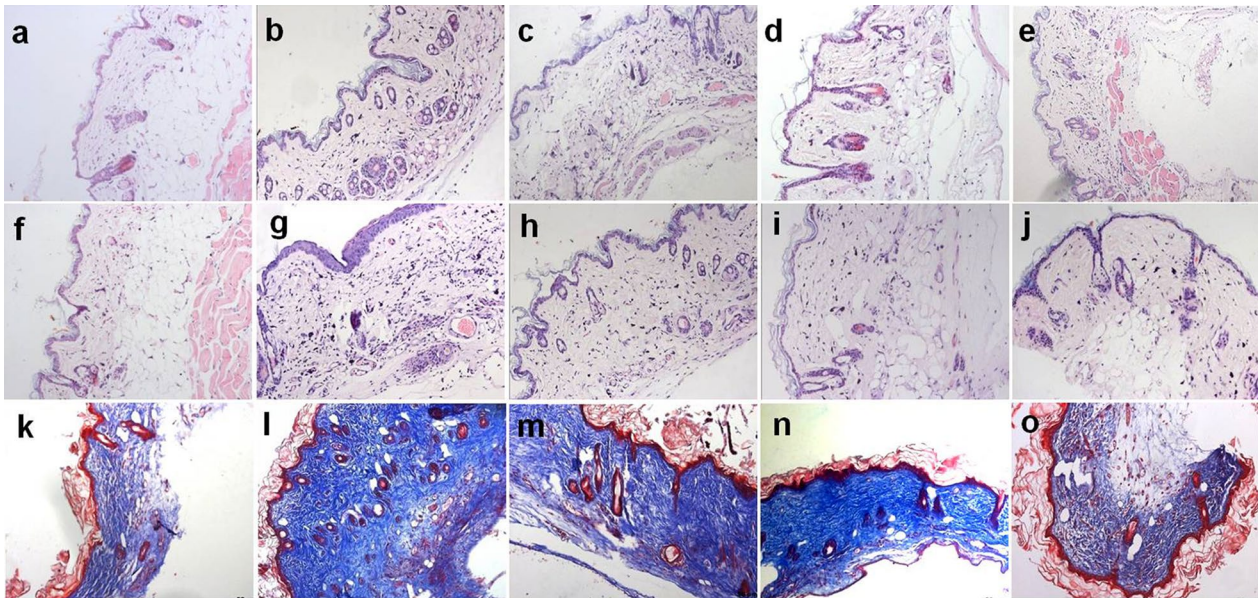


**Fig. 2** H<sub>2</sub>S improves pathological changes of skin tissues in BLM-induced mice ( $\times 200$ ). **a-j** HE stain; **k-o** Masson stain. **a-e** 7-day group; **f-o** 42-day group; **a, f, k** In the control group, the skin tissues had proper thickness and clear structure; **b, g, l** In the 7-day and 42-day model group, skin tissues points exhibited significant thickening of the dermis and disordered structure with increasing model establishment time; **c, h, m** and **d, i, n** In the low and high dose treatment group, the skin tissues exhibited a clear structure, the dermis became thinner, the lipid layer thickened, inflammatory cell filtration and collagen deposition significantly decreased compared to the model group; **e, j, o** Repeated injections of NaHS had little effect compared with the control group

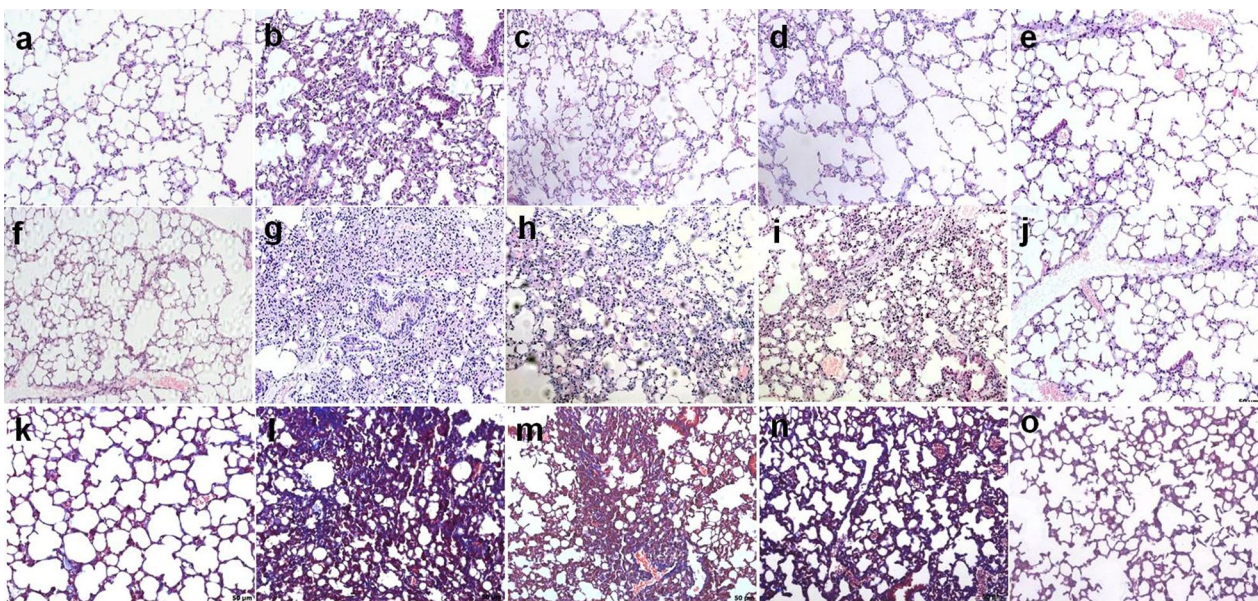


**Fig. 3** H<sub>2</sub>S improves pathological changes of lung tissues in BLM-induced mice ( $\times 200$ ). **a-j** HE stain; **k-o** Masson stain. **a-e** 7-day group; **f-o** 42-day group; **a, f, k** In the control group, the lung tissues were transparent and bright; **b, g, l** In the 7-day and 42-day model group, points all exhibited obvious inflammatory cell infiltration, disordered structure, increased collagen deposition, and thickening of alveolar septa; **c, h, m** and **d, i, n** In the low and high dose treatment group, the above targets significantly improved. **e, j, o** Repeated injections of NaHS had no significant effect on pathological changes of lung tissues

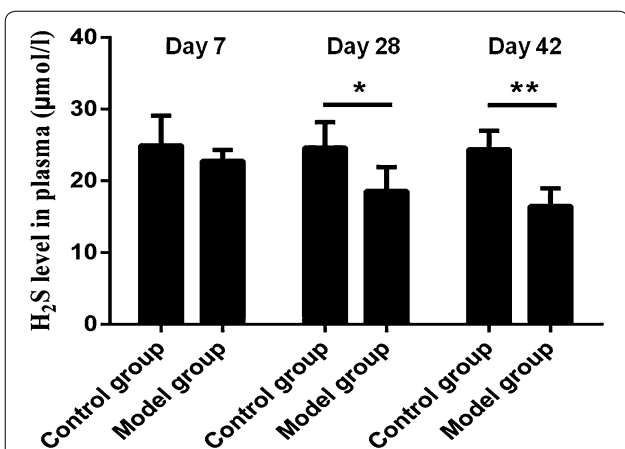


**Fig. 4** Changes in the plasma H<sub>2</sub>S concentrations. Compared to the control group, the plasma H<sub>2</sub>S concentrations for mice in the model group at different time points all decreased. Results represent mean ± SD of three independent experiments. \*P < 0.05 versus untreated group; \*\*P < 0.01 versus untreated group

was more evident than that in the low dose treatment group, but the difference was not statistically significant (Fig. 5).

**H<sub>2</sub>S inhibits the expression of α-SMA, Col-I, Col-III and FN in lung tissues on the 42th day**

Compared to that in the control group, the mRNA expression levels of α-SMA, Col-I, and Col-III in the lung

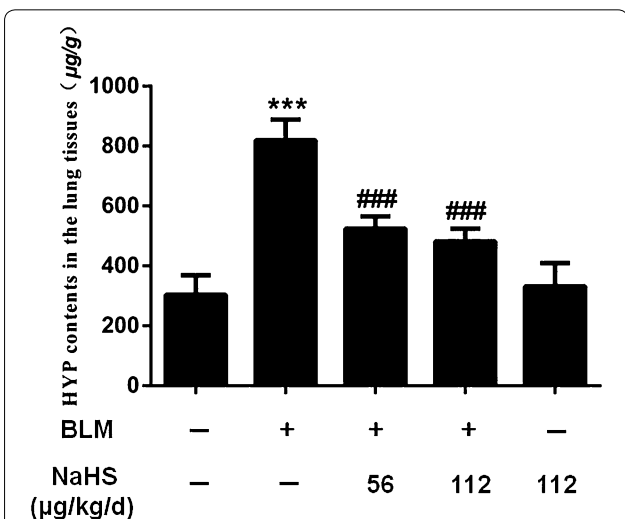


**Fig. 5** H<sub>2</sub>S reduces the expression level of HYP in the lung tissues of mice induced by BLM on the 42th day. Compared to the control group, the model group points significantly increased; After NaHS intervention, the HYP concentration in the treatment group significantly decreased. The decreasing trend in the high dose treatment group was more evident than that in the low dose treatment group. Data are presented as the mean ± SD. \*\*\*P < 0.001 versus control group. ###P < 0.001 versus model group

tissues of mice in the model group at different time points were significantly upregulated. For example in the 42-day group, after NaHS intervention, the expression levels of the above indicators for mice in the treatment group were significantly downregulated, and the differences were statistically significant. The trend of downregulation in the high dose treatment group was more evident than that in the low dose treatment group, but the difference was not statistically significant (Fig. 6).

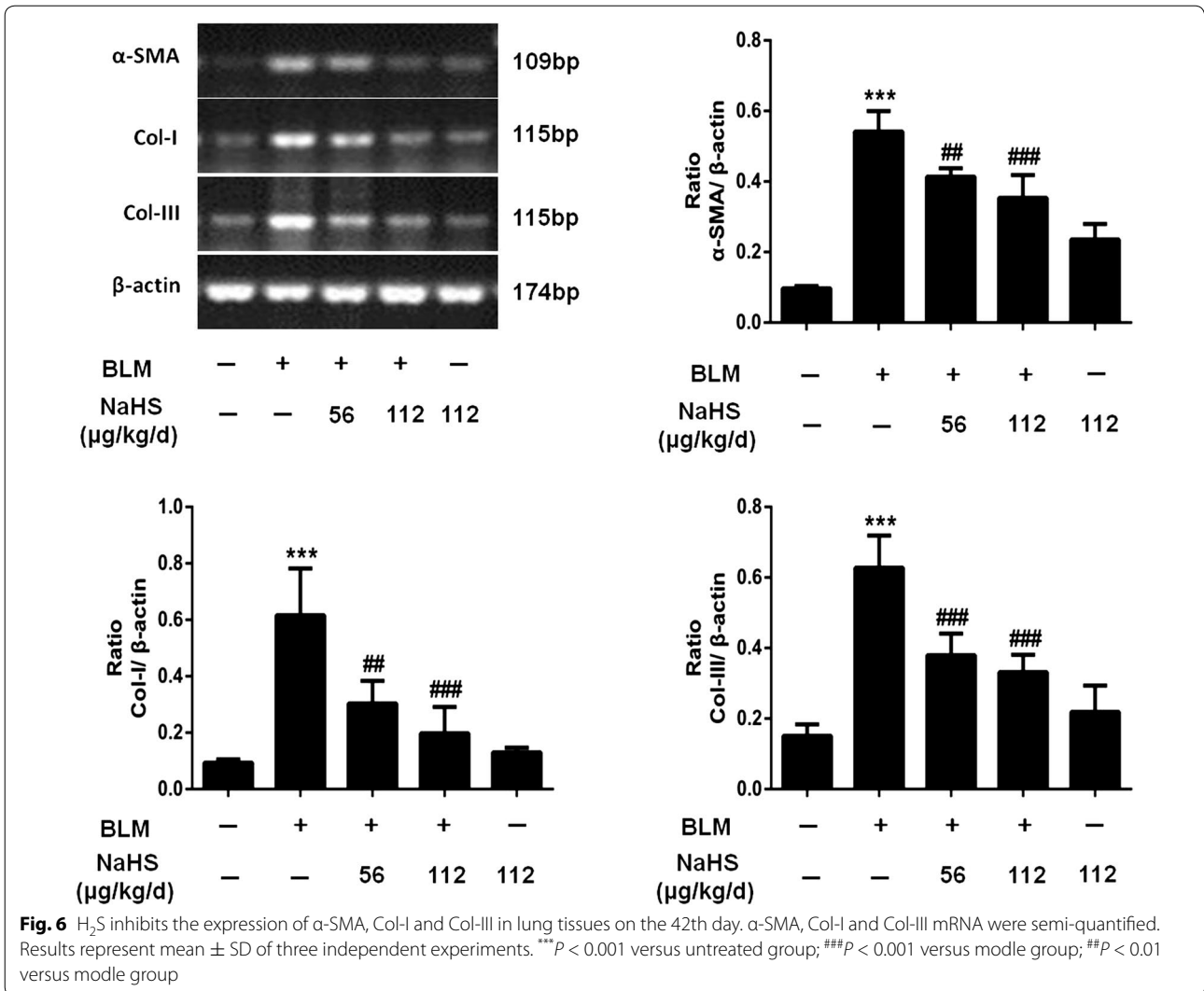
Compared to that in the control group, the protein expression levels of α-SMA and FN in the lung tissues of mice in the model group were significantly upregulated, and in the 42-day group after NaHS intervention, the expression levels of the above indicators for mice in the treatment group were significantly downregulated, and the differences were statistically significant. Compared to that in the low dose treatment group, the trend of downregulation of the expression levels of the above proteins in the high dose treatment group was more evident, but the difference was not statistically significant (Fig. 7).

**H<sub>2</sub>S reduces the number of ED-1-positive cells and MCP-1-positive cells in lung tissues on the 7th day**

Alveolitis was the most clearly observed in the 7-day model group. Therefore, the 7-day group was used for routine ED1 and MCP-1 immunohistochemistry to investigate the effects of H<sub>2</sub>S on inflammatory cytokines. The results of immunohistochemistry indicated that compared to the control group, the 7-day model group exhibited significant inflammatory cell infiltration and an increased number of ED1 and MCP-1 positive expression cells (Figs. 8b, 9b). After NaHS intervention, the expression levels of the above positive cells were significant downregulated (Figs. 8c, d, 9c, d). However, the difference between the low dose treatment group and the high dose treatment group was not statistically significant.

**H<sub>2</sub>S inhibits the expression of TGF-β1 and p-Smad2/3 in lung tissues on the 28th day and the 42th day**

Compared to the control group, the protein expression levels of TGF-β1 in lung tissues of mice in the model group at different time points were significantly upregulated, particularly the 28- and 42-day groups. After NaHS intervention, the protein expression level of TGF-β1 of mice in the treatment group was significantly downregulated, and the difference was statistically significant; however, the difference between the low dose treatment group and the high dose treatment group was not statistically significant. Meanwhile, compared to the control group, the protein expression levels of p-Smad2/3 in the 42 days model group lung tissues were significantly upregulated. After NaHS administration, the protein expression level of p-Smad2/3 in the treatment group was



significantly downregulated, and the difference was statistically significant (Fig. 10).

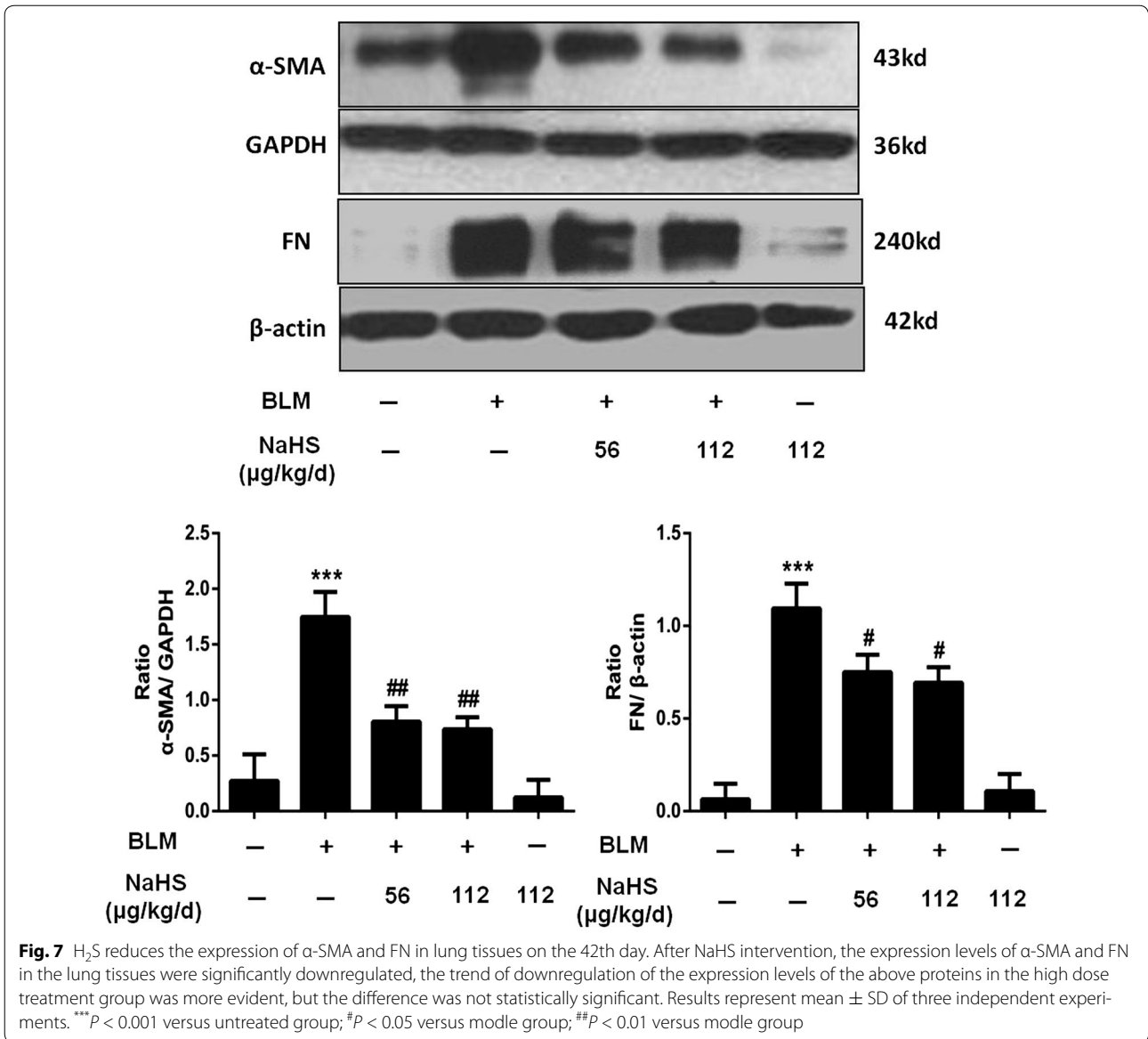
### Discussion

The present study demonstrated that inflammatory cell infiltration in skin and lung tissues increases and the synthesis of fibrogenic cytokines increases in a BLM-induced SSc mice model. Previous studies have suggested that exogenous H<sub>2</sub>S exerted a protective effect of pulmonary fibrosis by attenuating lipid peroxidation injury (Fang et al. 2009). And this study confirmed that exogenous H<sub>2</sub>S could relieve SSc through an anti-inflammation and anti-fibrosis mechanism, which provided a novel therapeutic approach to SSc.

In the present study, the mice model of SSc was established by subcutaneous injection of BLM. Consistent with previous studies (Yamamoto and Nishioka 2002;

Yamamoto et al. 1999), we could observe the destruction of the structure of skin and lung tissues, such as disordered structure, increased inflammatory cell infiltration, collagen deposition, significant skin and pulmonary fibrosis in mice from the model group at different time points. Furthermore, studies confirmed that the skin and lung tissues of SSc mice exhibited increased inflammatory cell filtration and upregulation of TGF-β1 expression at the early stage (Bienkowski and Gotkin 1995; Bonniaud et al. 2005). This study confirmed that BLM could induce inflammatory cell filtration and increase of the expression of fibrogenic factors in skin and lung tissues, these findings were consistent with previous studies indicated that the SSc mice model induced by BLM in this study was successfully established.

The relation of H<sub>2</sub>S and SSc associated fibrosis is not well defined. The results of this study suggested that the

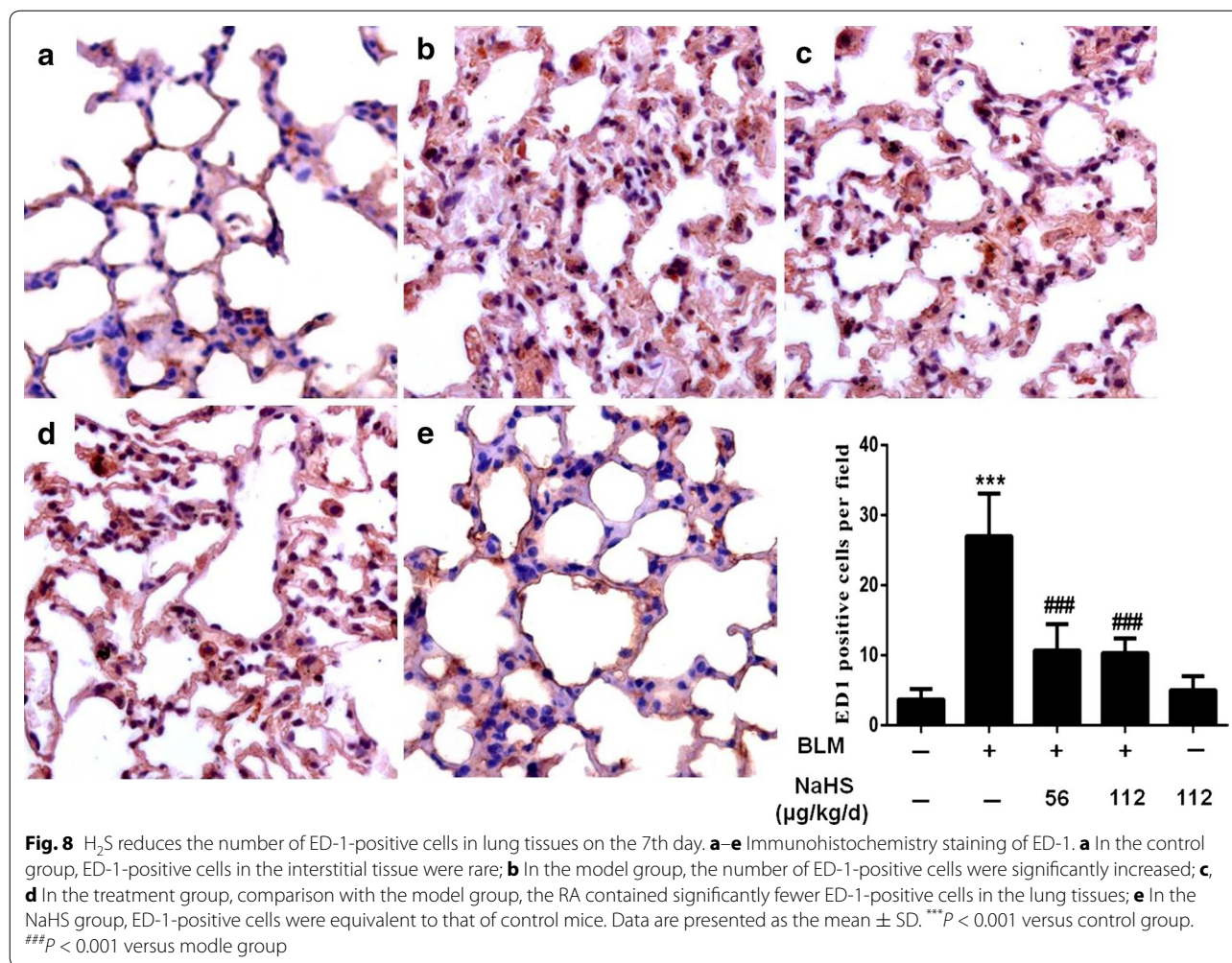


plasma H<sub>2</sub>S levels are decreased in the model group after subcutaneous injection of BLM. Which was consistent with the conclusion of previous studies showing that “organ fibrosis might be associated with H<sub>2</sub>S deficiency” (El-Seweidy et al. 2011; Tan et al. 2011). Therefore, we investigate the role of H<sub>2</sub>S on SSc-associated skin and lung fibrosis.

Our study indicate that H<sub>2</sub>S exhibited an anti-inflammatory property by reducing macrophage recruitment in lung tissues. The inflammatory cytokines such as ED-1 and MCP-1 were downregulated by NaHS in the 7-day

group. Substantial data have suggested that H<sub>2</sub>S is protective against inflammation in multiple fibrosis-related diseases (Babaei-Karamshahlo et al. 2012; Huang et al. 2012; Lu et al. 2015; Song et al. 2014; Whiteman and Winyard 2011). Our team previous study indicated that administration at a relatively low dose (56  $\mu$ g/kg/d) exogenous H<sub>2</sub>S could inhibit renal interstitial mononuclear cell infiltration and TNF- $\alpha$  expression in a unilateral ureteral obstructive (UUO) model, suggesting that H<sub>2</sub>S could exert its anti-inflammation function through the inhibition of the activation of macrophages (Song et al.

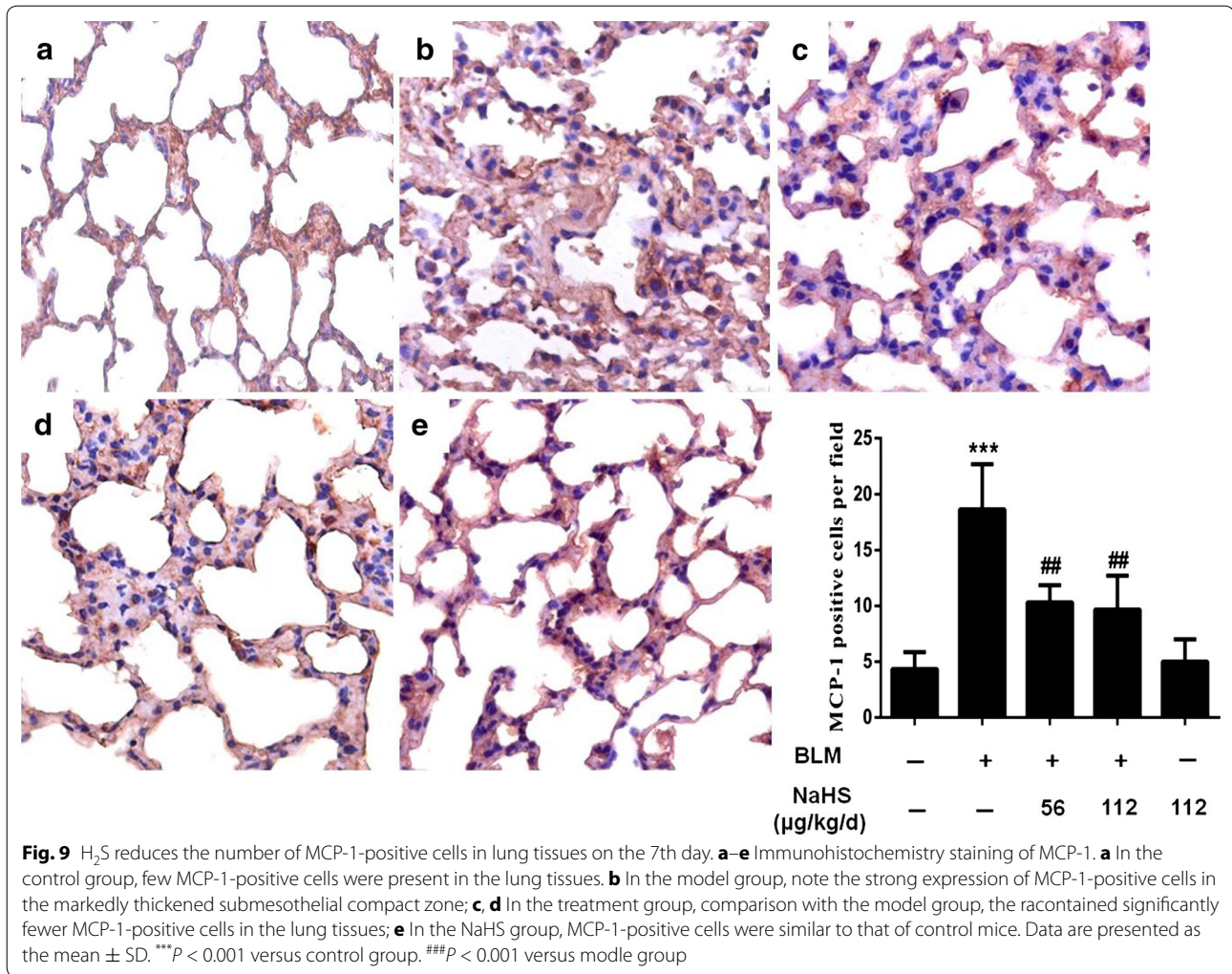




2014). Therefore, we speculated that the anti-pulmonary fibrosis function of H<sub>2</sub>S was associated with its anti-inflammation function. Inflammation plays an important role at the initial stage of systemic sclerosis, and inflammatory cell infiltration is the upstream event and one of the significant pathological features of organ fibrosis. The above study indicated that H<sub>2</sub>S inhibits the progression of skin and lung fibrosis through its anti-inflammation function.

In addition to the factor of inflammatory reaction, cytokines particular TGF-β1 also play an important role in the occurrence and development of fibrosis diseases (Flanders and Burmester 2003; Pittet et al. 2001). Substantial data have demonstrated that TGF-β1 promotes the transdifferentiation of fibroblasts into myofibroblasts (Scotton and Chambers 2007). Our results showed that

NaHS reduced the expression level of HYP and suppressed mRNA and protein expressions of α-SMA, FN, Col-1 and Col-3 induced by BLM in the lung tissues. Importantly, NaHS also attenuated the protein expressions of TGF-β1 at 28 and 42 days. These data suggested that H<sub>2</sub>S inhibited the fibroblast differentiation and extracellular matrix production partially by blocking the expression of TGF-β1. It is well known that TGF-β1 to be working main through its signal protein p-Smad2/3. Our study showed that after NaHS administration, the protein expression level of p-Smad2/3 in the treatment group was significantly downregulated on day 42. These results consistent with the previous study (Bei et al. 2013). This finding suggests that the anti-fibrotic effect of H<sub>2</sub>S may be connected with its inhibition of TGF-β/Smads pathway.



The above study confirmed that exogenous H<sub>2</sub>S had a protective function on SSc-related organ fibrosis. And importantly the present of H<sub>2</sub>S in a variety of mammalian tissues and organs support it may be without overt adverse effect. However, currently acquirable H<sub>2</sub>S donors like NaHS used in present study are not suitable for therapy because they release H<sub>2</sub>S uncontrolled. Tries are being made to obtain more appropriate H<sub>2</sub>S precursors for therapeutic aim. GYY4137 and SG1002 are two administrated H<sub>2</sub>S-releasing compounds that have been proven to be beneficial in various diseases such as hepatocellular carcinoma, diabetes, and chronic heart failure (Kondo et al. 2013; Lu et al. 2014; Wei et al. 2014). Such

compounds may become useful for treatment of SSc-related organ fibrosis.

### Conclusions

In conclusions, this study confirmed that H<sub>2</sub>S could improve SSc-related organ fibrosis. The mechanism was achieved through the inhibition of the inflammatory reaction and the reduction of TGF-β1 expression, thus reducing the accumulation of extracellular matrix. This study provides new insight into the treatment of SSc-related organ fibrosis in the clinic. A detailed understanding of the molecular mechanism and the related cell signalling pathways still awaits further study.

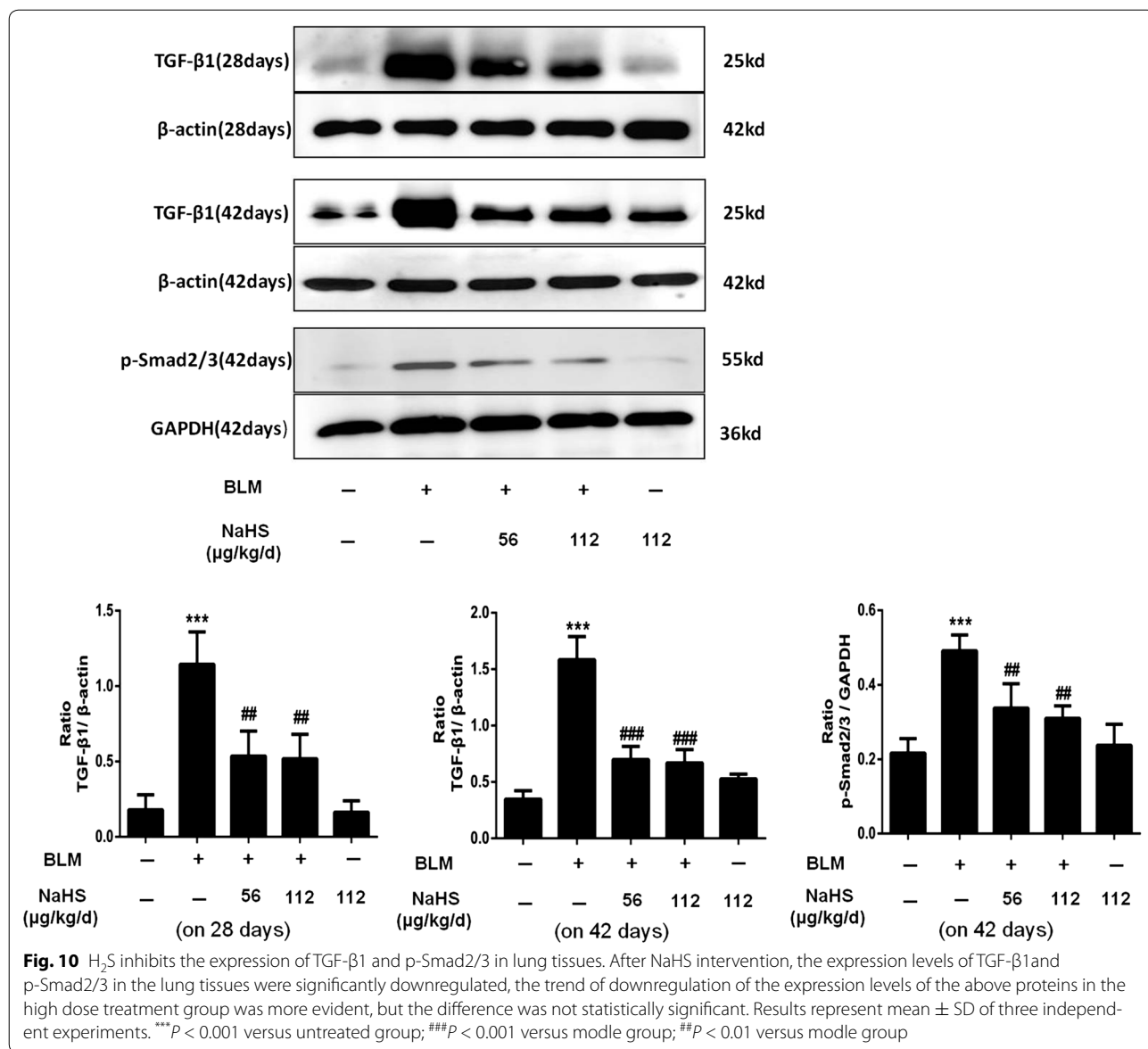


**Fig. 10** H<sub>2</sub>S inhibits the expression of TGF-β1 and p-Smad2/3 in lung tissues. After NaHS intervention, the expression levels of TGF-β1 and p-Smad2/3 in the lung tissues were significantly downregulated, the trend of downregulation of the expression levels of the above proteins in the high dose treatment group was more evident, but the difference was not statistically significant. Results represent mean ± SD of three independent experiments. \*\*\**P* < 0.001 versus untreated group; ###*P* < 0.001 versus modle group; ##*P* < 0.01 versus modle group

**Authors' contributions**

ZW participated in conception, design, acquisition, analysis and interpretation of data and drafted the manuscript. XYY participated in acquisition of data and samples, analysis and interpretation of data and drafted the manuscript. LYG and SF participated in design, statistical analysis and interpretation of data. KS, LYL and YL participated in analysis and interpretation of data and were also involved in drafting the manuscript and revising it. HYS participated in conception, design, analysis and interpretation of data and was also involved in drafting the manuscript and revising it. All authors read and approved the final manuscript.

**Acknowledgements**

This work was supported by grants from the National Nature Science Foundation of China (81302584, 81400762 and 81200495).

**Competing interests**

The authors declare that they have no competing interests.

**Ethical standard**

The authors can confirm that they have read and understood the contents of the section on compliance with ethical standards of the journal. The study complies with current animal rights and ethical consideration.

Received: 11 April 2016 Accepted: 6 July 2016

Published online: 15 July 2016

**References**

Babaei-Karamshahlou M, Hooshmand B, Hajizadeh S, Mani AR (2012) The role of endogenous hydrogen sulfide in pathogenesis of chronotropic dysfunction in rats with cirrhosis. *Eur J Pharmacol* 696:130–135  
 Bei Y, Hua-Huy T, Duong-Quy S, Nguyen VH, Chen W, Nicco C, Batteux F, Dinh-Xuan AT (2013) Long-term treatment with fasudil improves bleomycin-induced pulmonary fibrosis and pulmonary hypertension via inhibition of Smad2/3 phosphorylation. *Pulm Pharmacol Ther* 26:635–643  
 Bienkowski RS, Gotkin MG (1995) Control of collagen deposition in mammalian lung. *Proc Soc Exp Biol Med Soc Exp Biol Med* 209:118–140  
 Bonniaud P, Margetts PJ, Kolb M, Schroeder JA, Kapoun AM, Damm D, Murphy A, Chakravarty S, Dugar S, Higgins L et al (2005) Progressive transforming growth factor beta1-induced lung fibrosis is blocked by an orally active ALK5 kinase inhibitor. *Am J Respir Crit Care Med* 171:889–898

- El-Seweidy MM, Sadik NA, Shaker OG (2011) Role of sulfurous mineral water and sodium hydrosulfide as potent inhibitors of fibrosis in the heart of diabetic rats. *Arch Biochem Biophys* 506:48–57
- Fang L, Li H, Tang C, Geng B, Qi Y, Liu X (2009) Hydrogen sulfide attenuates the pathogenesis of pulmonary fibrosis induced by bleomycin in rats. *Can J Physiol Pharmacol* 87:531–538
- Flanders KC, Burmester JK (2003) Medical applications of transforming growth factor-beta. *Clin Med Res* 1:13–20
- Gao C, Xu DQ, Gao CJ, Ding Q, Yao LN, Li ZC, Chai W (2012) An exogenous hydrogen sulphide donor, NaHS, inhibits the nuclear factor kappaB inhibitor kinase/nuclear factor kappaB inhibitor/nuclear factor-kappaB signaling pathway and exerts cardioprotective effects in a rat hemorrhagic shock model. *Biol Pharm Bull* 35:1029–1034
- Huang J, Wang D, Zheng J, Huang X, Jin H (2012) Hydrogen sulfide attenuates cardiac hypertrophy and fibrosis induced by abdominal aortic coarctation in rats. *Mol Med Rep* 5:923–928
- Kondo K, Bhushan S, King AL, Prabhu SD, Hamid T, Koenig S, Murohara T, Predmore BL, Gojon G Sr, Gojon G Jr et al (2013) H(2)S protects against pressure overload-induced heart failure via upregulation of endothelial nitric oxide synthase. *Circulation* 127:1116–1127
- Li T, Zhao B, Wang C, Wang H, Liu Z, Li W, Jin H, Tang C, Du J (2008) Regulatory effects of hydrogen sulfide on IL-6, IL-8 and IL-10 levels in the plasma and pulmonary tissue of rats with acute lung injury. *Exp Biol Med* 233:1081–1087
- Lu S, Gao Y, Huang X, Wang X (2014) GYY4137, a hydrogen sulfide (H(2)S) donor, shows potent anti-hepatocellular carcinoma activity through blocking the STAT3 pathway. *Int J Oncol* 44:1259–1267
- Lu Y, Gao L, Li L, Zhu Y, Wang Z, Shen H, Song K (2015) Hydrogen sulfide alleviates peritoneal fibrosis via attenuating inflammation and TGF-beta1 synthesis. *Nephron* 131:210–219
- Moody BF, Calvert JW (2011) Emergent role of gasotransmitters in ischemia-reperfusion injury. *Med Gas Res* 1:3
- Pittet JF, Griffiths MJ, Geiser T, Kaminski N, Dalton SL, Huang X, Brown LA, Gotwals PJ, Kotliansky VE, Matthay MA et al (2001) TGF-beta is a critical mediator of acute lung injury. *J Clin Invest* 107:1537–1544
- Scotton CJ, Chambers RC (2007) Molecular targets in pulmonary fibrosis: the myofibroblast in focus. *Chest* 132:1311–1321
- Song K, Wang F, Li Q, Shi YB, Zheng HF, Peng H, Shen HY, Liu CF, Hu LF (2014) Hydrogen sulfide inhibits the renal fibrosis of obstructive nephropathy. *Kidney Int* 85:1318–1329
- Tan G, Pan S, Li J, Dong X, Kang K, Zhao M, Jiang X, Kanwar JR, Qiao H, Jiang H et al (2011) Hydrogen sulfide attenuates carbon tetrachloride-induced hepatotoxicity, liver cirrhosis and portal hypertension in rats. *PLoS ONE* 6:e25943
- Vandiver M, Snyder SH (2012) Hydrogen sulfide: a gasotransmitter of clinical relevance. *J Mol Med* 90:255–263
- Walker KM, Pope J, Participating members of the Scleroderma Clinical Trials C, Canadian Scleroderma Research, G (2012) Treatment of systemic sclerosis complications: what to use when first-line treatment fails—a consensus of systemic sclerosis experts. *Semin Arthritis Rheum* 42:42–55
- Wang R (2012) Shared signaling pathways among gasotransmitters. *Proc Natl Acad Sci USA* 109:8801–8802
- Wei WB, Hu X, Zhuang XD, Liao LZ, Li WD (2014) GYY4137, a novel hydrogen sulfide-releasing molecule, likely protects against high glucose-induced cytotoxicity by activation of the AMPK/mTOR signal pathway in H9c2 cells. *Mol Cell Biochem* 389:249–256
- Whiteman M, Winyard PG (2011) Hydrogen sulfide and inflammation: the good, the bad, the ugly and the promising. *Exp Rev Clin Pharmacol* 4:13–32
- Yamamoto T, Nishioka K (2002) Animal model of sclerotic skin. V: increased expression of alpha-smooth muscle actin in fibroblastic cells in bleomycin-induced scleroderma. *Clin Immunol* 102:77–83
- Yamamoto T, Takagawa S, Katayama I, Yamazaki K, Hamazaki Y, Shinkai H, Nishioka K (1999) Animal model of sclerotic skin. I: local injections of bleomycin induce sclerotic skin mimicking scleroderma. *J Invest Dermatol* 112:456–462

Submit your manuscript to a SpringerOpen® journal and benefit from:

- Convenient online submission
- Rigorous peer review
- Immediate publication on acceptance
- Open access: articles freely available online
- High visibility within the field
- Retaining the copyright to your article

Submit your next manuscript at ► [springeropen.com](http://springeropen.com)